EFFECT OF CRACK BLUNTING ON THE DUCTILE-BRITTLE RESPONSE OF CRYSTALLINE MATERIALS

D.M.LIPKIN,* G.E.BELTZ,** and L.L.FISCHER**
*Physical Metallurgy Laboratory, GE Research & Development Center, Niskayuna, NY 12309
**Department of Mechanical and Environmental Engineering, University of California, Santa Barbara, CA 93106-5070

ABSTRACT

We propose a self-consistent criterion for crack propagation versus dislocation emission, taking into account the effects of crack-tip blunting. Continuum concepts are used to evaluate the evolving competition between crack advance and dislocation nucleation as a function of crack-tip curvature. This framework is used to classify crystals as intrinsically ductile or brittle in terms of the unstable stacking energy, the surface energy, and the peak cohesive stresses achieved during opening and shear of the atomic planes. We find that ductile-brittle criteria based on the assumption that the crack is ideally sharp capture only two of the four possible fracture regimes. One implication of the present analysis is that a crack may initially emit dislocations, only to reinitiate cleavage upon reaching a sufficiently blunted crack-tip geometry.

INTRODUCTION

Ductile versus brittle behavior of crystalline materials is among the least understood of the fundamental mechanical phenomena in materials science. The conventional procedure for applying continuum-based theories to predict the mechanical response of cracked bodies is to assume that the crack is atomically sharp, then to analyze how the body responds to an applied load. Rice and Thomson [1] instituted this approach by comparing the load required to propagate the crack with the load necessary to emit a dislocation on a slip plane inclined to the crack plane and intersecting the crack front (see Figure 1). If dislocation emission occurs at a load lower than that required for crack propagation, then the material is said to be "intrinsically" ductile; otherwise, it is said to be "intrinsically" brittle. This type of physical modeling has evolved considerably over the years to account for factors such as nonlinear defect core structures, realistic slip systems, and three-dimensional dislocation configurations [2]; however, the role of crack blunting when dislocation emission initially occurs has received extremely limited attention [3-7]. Atomistic studies [4,5] agree on one major point: the favorability of crack advance versus dislocation emission can change when the crack tip blunts. Therefore, a crystal should not be classified as intrinsically ductile or brittle based on the emission of the first dislocation.

Presently, we consider the ongoing competition between crack propagation and subsequent dislocation nucleation as the crack-tip curvature evolves toward steady state. We identify the key material parameters that govern the outcome of this competition, allowing a reassessment of the fundamental ductile-brittle response of crystalline materials.

Mat. Res. Soc. Symp. Proc. Vol. 539 ©1999 Materials Research Society

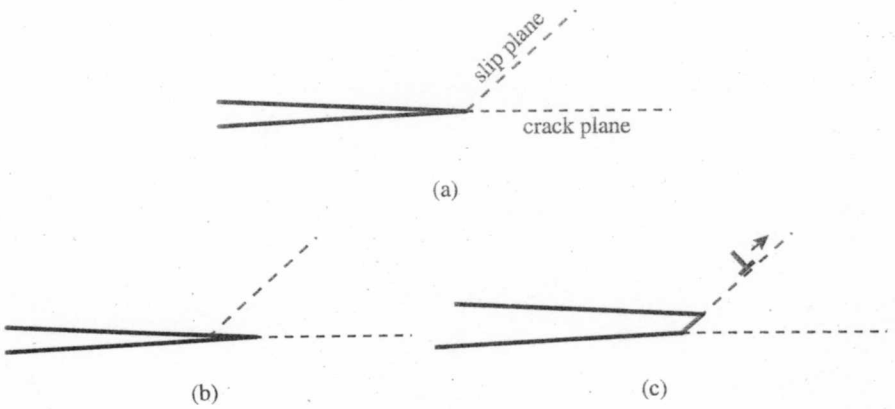

Fig.1 Illustration of the competition between dislocation emission and cleavage decohesion at an initially sharp crack tip with an intersecting slip plane. (a) The starting crack configuration leads to either (b) crack-tip bond rupture or (c) dislocation emission and consequent crack-tip blunting.

MODEL

We first consider crack propagation. According to the Griffith theory [8], a sharp crack will advance when the applied energy release rate, $\mathcal{G}$, attains $2\gamma_s$, the energy per unit area required to create two free surfaces. Formally, $\mathcal{G}$ is the rate of decrease of stored elastic energy in the system per unit area of crack advance. $\mathcal{G}$ scales directly with the intensity of loads applied to the body and is related to the stress intensity factor, K, by the Irwin relation [9]

$$\mathcal{G} = \frac{\left(1-\nu^2\right) K^2}{E} \qquad (1)$$

where E is Young's modulus and ν is Poisson's ratio. For illustration, we consider pure mode I loading, wherein the symmetry of the applied load is such that the crack faces tend to open rather than shear against one another (the formalism can readily be extended to mixed-mode loading). The material parameter $2\gamma_s$ is graphically depicted in Figure 2 as the area under the stress versus displacement curve for the atomic planes undergoing separation during the fracture process. In the Griffith theory, the critical applied load for fracture does not depend on σ_p, the maximum of the stress vs. separation curve, but only on the area underneath it. This lack of dependence on σ_p is also borne out by cohesive zone models [10].

We envision a crack that is capable of blunting on the atomic scale in response to the applied load. The crack-tip blunting can represent either purely elastic deformation or dislocation emission on slip planes intersecting the crack front. A slender elliptical slit is used to approximate the blunting crack (Figure 2). The approximation of the crack as an ellipse not

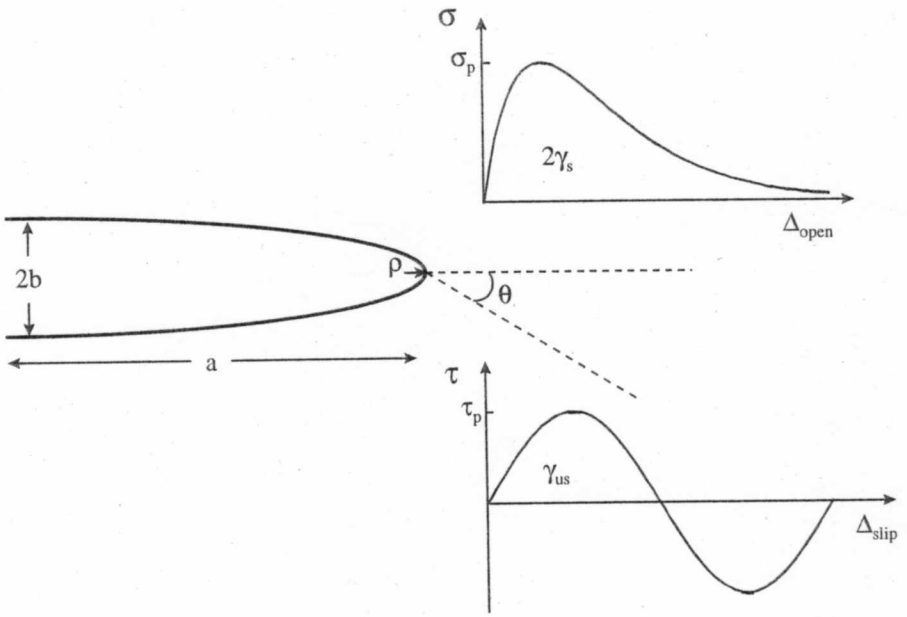

Fig.2 The blunted crack configuration is approximated as an elliptical slit having a major axis of length 2a and a minor axis of length 2b. The crack-tip curvature is $\rho=b^2/a$. On the crack plane, the opening displacement, Δ_{open}, adheres to a traction-separation law, $\sigma(\Delta_{open})$, schematically illustrated in (a). Along the slip plane inclined by an angle θ to the crack plane, the slip displacement, Δ_{slip}, adheres to the Peierls-like relationship, $\tau(\Delta_{slip})$, illustrated in (b). $2\gamma_s$ and γ_{us} correspond to the areas under the opening and shear traction curves, respectively.

only makes our calculations tractable, but it also introduces a length scale, ρ (radius of curvature of the tip), into the analysis. The elliptical crack-tip profile represents a drastic departure from the sharp corner (and its associated stress singularity) that would result, from a continuum viewpoint, when dislocations emit along a single slip plane (e.g., Figure 1c). The angled crack tip (which does retain a sharp corner) has received some attention in the literature, notably from Schiøtz et al. [4]. However, atomistic simulations by Gumbsch [5] suggest that, at the atomic scale, it makes little sense to exploit a shape that contains a stress singularity in the continuum description.

We now consider an infinite, two-dimensional, solid containing an elliptical cut-out having a major axis of length 2a and a minor axis of length 2b (Figure 2). A remote tensile stress of magnitude σ_∞ is applied perpendicular to the major axis. The radius of curvature at the

tip, ρ, is equal to b^2/a. The elasticity solution for this problem, given by Inglis [11] and Muskhelishvili [12], predicts that the stress at the crack tip is

$$\sigma_{tip} = \sigma_\infty\left(1+\frac{2a}{b}\right) = \sigma_\infty\left(1+2\sqrt{\frac{a}{\rho}}\right) \qquad (2)$$

Assuming the crack is not sharp (and thereby departing from the Griffith theory), we impose the condition that the crack propagates in a brittle fashion when the local stress given by Equation (2) achieves the cohesive strength of the solid, σ_p. To a remote observer who sees the cut-out simply as a finite crack, the stress intensity factor is $K_I = \sigma_\infty\sqrt{\pi a}$ [13]. Combining Equations (1) and (2) and solving for the critical energy release rate leads to

$$\mathcal{J}_{cleave} = \frac{\pi\sigma_p^2}{E'\left(\frac{1}{\sqrt{a}}+\frac{2}{\sqrt{\rho}}\right)^2} \approx \frac{\pi\sigma_p^2\rho}{4E'} \qquad (3)$$

where $E' \equiv E/(1-\nu^2)$ for plane strain. We have used the approximation in Equation (3) that $\rho << a$, i.e., the crack is of some macroscopic, "laboratory" dimension, while ρ is of atomic dimension. Although Equation (3) is linear in ρ, it is expected to break down as ρ approaches zero. In order to maintain a finite toughness in the ideally sharp crack limit, the Griffith theory must prevail as ρ becomes vanishingly small. For ρ approaching zero, the applied energy release rate for crack advance must approach the Griffith limit, $2\gamma_s$. For larger values of ρ, $\mathcal{J}_{cleave}$ should asymptotically approach the straight line given by Equation (3). This is indicated schematically in Figure 3. The transition zone between the two limits has been assumed to be smooth. However, detailed mechanical analyses of the exact form of $\mathcal{J}_{cleave}(\rho)$, using realistic relations to represent the stress vs. separation curves of Figure 2, are in progress, and initial results confirm the basic behavior indicated in Figure 3 [14].

The crossover curvature, below which blunting effects are superseded by the Griffith limit, is $8\gamma_s E'/\pi\sigma_p^2$. This crossover appears to be consistent with atomistic results given by Schiøtz et al. [4] and Gumbsch [5], who found that only moderate increases in crack initiation load above the Griffith limit are noted for slight excursions from an ideally sharp crack tip. In the latter study, more significant increases in the failure thresholds were noted for significantly blunter cracks.

Dislocation nucleation follows an analogous treatment to that presented for cleavage. Recently, Rice and coworkers [15,16] provided an analysis of the threshold load for dislocation nucleation. They considered a slip plane intersecting a sharp crack. The slip plane was taken to obey an interplanar potential associated with rigid block sliding in a homogeneous lattice (Figure 2). The principal result is that the critical applied $\mathcal{J}$ (the prevailing energy release rate if the crack were to move as a classical singular crack, without a shear or decohesion zone at its tip) associated with dislocation nucleation is

$$\mathcal{G}_{disl} = \frac{8\gamma_{us}}{(1+\cos\theta)\sin^2\theta} \equiv g(\theta)\,\gamma_{us} \qquad (4)$$

where θ is the inclination of the slip plane with respect to the crack plane. Equation (4) assumes the Burgers vector lies completely within the plane of Figure 2 (i.e. has no component parallel to the crack front) and overestimates $\mathcal{G}_{disl}$ for $\theta > 0$ because it ignores shear-tension coupling (i.e., the effects of tension normal to the slip plane) and uses an approximate stress solution on inclined slip planes [15-17]. The crack-tip shear stress, $\sigma_{r\theta}$, along the inclined slip plane is given approximately by

$$\tau_{tip} \approx \sigma_\infty \left(1 + 2\sqrt{\frac{a}{\rho}}\right) \sin\theta\cos\theta \qquad (5)$$

which is essentially Equation (2) scaled by the appropriate Schmidt Factor. Equation (5) is valid for slip plane inclination angles up to about 70°, beyond which the equation breaks down because the maximum shear stress does not occur directly at the crack tip. Equating (5) with the peak shear stress, τ_p, and solving for the critical applied energy release rate for dislocation nucleation gives

$$\mathcal{G}_{disl} \approx \frac{\pi\tau_p^2\rho}{4E'\sin^2\theta\cos^2\theta} \qquad (6)$$

Although $\mathcal{G}_{disl}$ scales linearly with ρ, the relation must not be interpreted physically for ρ approaching zero, whereupon the dislocation nucleation criterion is given by Equation (4). The transition in $\mathcal{G}_{disl}$ from Equation (4) to Equation (6) is again assumed to be smooth, as shown in Figure 3. The crossover crack-tip curvature is approximately $32\gamma_{us}E'\cos^2\theta / \pi\tau_p^2(1+\cos\theta)$.

DISCUSSION

Based upon the threshold criteria derived above, we can now differentiate between an intrinsically ductile and an intrinsically brittle crystal. Imagine a material with an initially sharp crack. Knowing the parameters $2\gamma_s$, γ_{us}, σ_p, and τ_p (and elastic moduli), plots of $\mathcal{G}_{disl}$ and $\mathcal{G}_{cleave}$ vs. ρ can be constructed, which can follow one of only four possibilities, as indicated in Figure 3:

Case (i): As depicted in Figure 3(a), $2\gamma_s$ is less than $g(\theta)\gamma_{us}$, and σ_p is less than $\tau_p/\sin\theta\cos\theta$. When the material is loaded, the crack advances by crack-tip cleavage. Because the condition for dislocation nucleation is never satisfied, no blunting (aside from the elastic relaxation, ρ_{el}) occurs, and we classify this material as intrinsically brittle. Many ceramics below their ductile-to-brittle transition temperature and glasses below their glass transition temperature would be expected to fall under this category.

Case(ii): As depicted in Figure 3(b), $2\gamma_s$ is less than $g(\theta)\gamma_{us}$, but σ_p is greater than $\tau_p/\cos\theta\sin\theta$, giving rise to a crossover between $\mathcal{G}_{disl}(\rho)$ and $\mathcal{G}_{cleave}(\rho)$. However, cleavage is

favored over dislocation nucleation, and an initially sharp crack remains sharp. This material is intrinsically brittle; however, it is evident that a pre-existing, sufficiently blunt crack could sustain ductile behavior and continue to blunt. The latter behavior is, however, metastable, as a perturbation in the local crack-tip curvature could cause it to spontaneously sharpen and proceed to extend via cleavage.

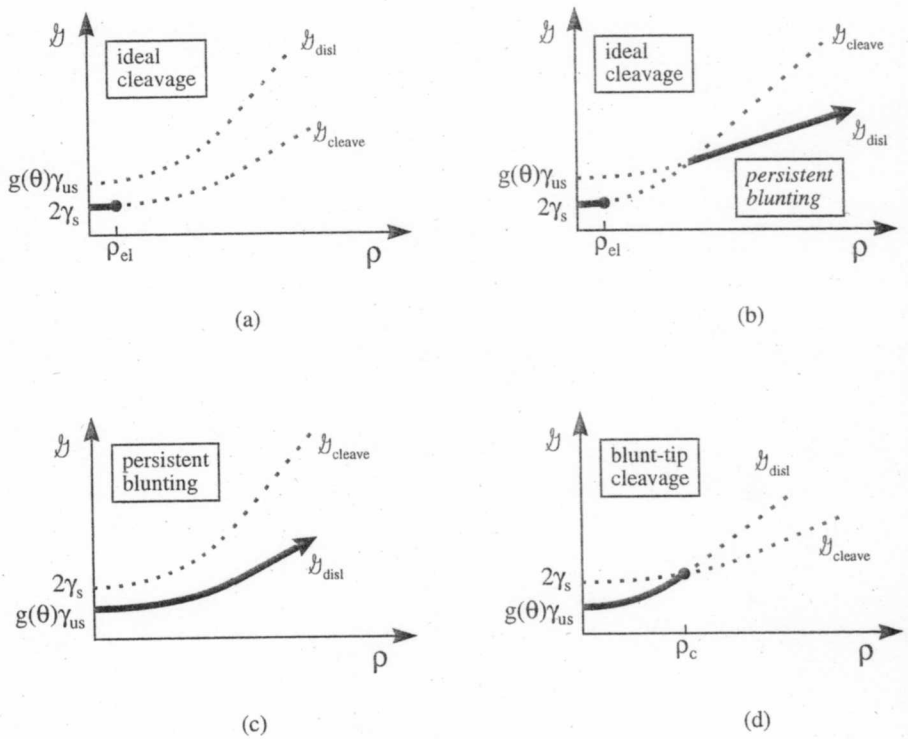

Fig.3 Four possible fracture regimes are anticipated by the present model. (a) Ideal cleavage, characterized by a Griffith fracture criterion and near-zero tip curvature, occurs when $2\gamma_s<g(\theta)\gamma_{us}$ and $\sigma_p<\tau_p/\sin\theta\cos\theta$. (b) Ideal cleavage with a metastable blunting regime occurs when $2\gamma_s<g(\theta)\gamma_{us}$ and $\sigma_p>\tau_p/\sin\theta\cos\theta$. The metastable regime is marked by the ability of a pre-blunted crack to continue blunting by persistent dislocation emission although sharp-tip cleavage is the more stable configuration. (c) Persistent blunting, characterized by repeated dislocation emission and consequent crack-tip blunting, occurs when $2\gamma_s>g(\theta)\gamma_{us}$ and $\sigma_p>\tau_p/\sin\theta\cos\theta$. (d) Blunt-tip cleavage, characterized by the cleavage of a finite-blunted crack, occurs when $2\gamma_s>g(\theta)\gamma_{us}$ and $\sigma_p<\tau_p/\sin\theta\cos\theta$.

Case(iii): As depicted in Figure 3(c), $g(\theta)\gamma_{us}$ is less than $2\gamma_s$ and $\tau_p/\sin\theta\cos\theta$ is less than σ_p. Now, dislocation nucleation is the preferred response to applied load. As the crack blunts and ρ continues to increase, $\mathcal{J}_{disl}$ remains less than $\mathcal{J}_{cleave}$, and persistent dislocation nucleation remains the preferred mode. Therefore, the material is classified as intrinsically ductile. Most fcc metals at room temperature are expected to fall under this regime.

Case(iv): As in the previous case, $g(\theta)\gamma_{us}$ is less than $2\gamma_s$, and initial dislocation nucleation is preferred. However, $\tau_p/\sin\theta\cos\theta$ is greater than σ_p and crossover occurs at a critical value of ρ, as shown in Figure 3(d). Therefore, when the crack tip blunts to a critical radius of curvature, cleavage becomes energetically more favorable than dislocation nucleation and the crack advances. This behavior is representative of what is believed to occur in some bcc metals and at certain metal-ceramic interfaces.

Although the present model extends our ability to predict the competition between cleavage and blunting beyond the first dislocation emission event, a number of issues remain to be resolved. The motion of surrounding dislocations in the crystal is not accounted for in this treatment, nor are three-dimensional aspects associated with dislocation nucleation on "oblique" slip planes that intersect the crack tip at a point rather than along a line. For the cases described above, in which dislocations are emitted from the crack tip, the applied energy release rates should rigorously be interpreted as those based on the local, or screened, crack-tip field, which can differ from the macroscopic field due to other dislocations, crystalline anisotropy, and various other local heterogeneities. Although emitted dislocations are assumed to be swept sufficiently far away that we may ignore these shielding effects, the importance of external dislocations and plastic dissipation on the ductile versus brittle competition have been shown to play a critical role in the actual applied loads necessary to maintain the "local" loads described in this paper [18-22]. This notion can be exploited to predict the macroscopic fracture toughness, as well as to explain the large dependence of ductile vs. brittle fracture energies on temperature, for example in [22].

Much work has been done on correlating γ_{us} and $2\gamma_s$ with observed fracture processes, especially in the area of numerical simulations of fracture. The present model highlights the relevance of the traction law parameters σ_p and τ_p. The determination of peak tensile stresses (e.g., in the spirit of Rose et al. [23]) and peak shear stresses (e.g,. as in the work by Cleri et al. [17]) and their role in the ductile versus brittle behavior of crystals should be assessed in future simulations and experiments on fracture.

REFERENCES

1. J. R. Rice and R. Thomson, *Philos. Mag.* **29**, 73 (1974).
2. G. Xu, A. S. Argon, and M. Ortiz, *Philos. Mag.* A **75**, 341 (1997).
3. G. J. Dienes and A. Paskin, *J. Phys. Chem. Solids* **48**, 1015 (1987).
4. J. Schiøtz, L. M. Canel, and A. E. Carlsson, *Phys. Rev. B* **55**, 6211 (1997).

5. P. Gumbsch, *J. Mater. Res.* **10**, 2897 (1995).

6. G. E. Beltz and L. L. Fischer, *Philos. Mag. A*, in press (1998).

7. J. Weertman, in *High Cycle Fatigue of Structural Materials*, edited by W. O. Soboyejo and T. S. Srivatsan (The Minerals, Metals, and Materials Society, 1997) pp. 41-48.

8. A. A. Griffith, *Philos. Trans. R. Soc. London A* **221**, 163 (1920).

9. G. R. Irwin, *J. Appl. Mech.* **24**, 361 (1957).

10. J. R. Rice and J.-S. Wang, *Mater. Sci. Eng. A* **107**, 23 (1989).

11. C. E. Inglis, *Trans. Institution of Naval Architects* **55**, 219 (1913).

12. N. I. Muskhelishvili, Some Basic Problems on the Mathematical Theory of Elasticity: Fundamental Equations, Plane Theory of Elasticity, Torsion and Bending (Noordhoff, 1975).

13. H. Tada, P. C. Paris, and G. R. Irwin, The Stress Analysis of Cracks Handbook (Del Research Corporation, St. Louis, 1985).

14. G. E. Beltz, D. M. Lipkin, and L. L. Fischer, *Appl. Phys. Lett.*, in press (1999).

15. J. R. Rice, *J. Mech. Phys. Solids* **40**, 239 (1992).

16. Y. Sun, G. E. Beltz, and J. R. Rice, *Mater. Sci. Eng. A* **170**, 67 (1993).

17. F. Cleri, S. Yip, D. Wolf, and S. R. Phillpot, *Phys. Rev. Lett.* **79**, 1309 (1997).

18. J. Weertman, *Acta Metall.* **26**, 1731 (1978).

19. R. Thomson, *J. Mater. Sci.* **13**, 128 (1978).

20. G. E. Beltz, J. R. Rice, C. F. Shih, and L. Xia, *Acta Materiala* **44**, 3943 (1996).

21. D. M. Lipkin and G. E Beltz, *Acta Materiala* **44**, 1287 (1996).

22. D. M. Lipkin, D. R. Clarke, and G. E. Beltz, *Acta Materiala* **44**, 4051 (1996).

23. J. H. Rose, J. R. Smith, and J. Ferrante, *Phys. Rev. B* **28**, 1835 (1983).